LAWRENCE
LIVERMORE
NATIONAL
LABORATORY

LLNL-CONF-411355

Radioactive Contraband Detection: A Bayesian Approach

J. Candy, E. Breitfeller, B. Guidry, D. Manatt, K. Sale, D. Chambers, M. Axelrod, A. Meyer

March 18, 2009

IEEE OCEANS '09
Bremen , Germany
May 11, 2009 through May 14, 2009

Radioactive Contraband Detection: A Bayesian Approach

J.V. Candy, *Fellow, IEEE*, E. Breitfeller, *Member, IEEE*, B. Guidry, *Member, IEEE*, D. Manatt, K. Sale, D. Chambers, *Senior Member, IEEE*, M. Axelrod and A. Meyer, *Senior Member, IEEE*

***Abstract*—Radionuclide emissions from nuclear contraband challenge both detection and measurement technologies to capture and record each event. The development of a sequential Bayesian processor incorporating both the physics of gamma-ray emissions and the measurement of photon energies offers a physics-based approach to attack this challenging problem. It is shown that a "physics-based" structure can be used to develop an effective detection technique, but also motivates the implementation of this approach using or particle filters to enhance and extract the required information.**

I. INTRODUCTION

Radionuclide detection is a critical first line defense to detect the transportation of radiological materials by potential terrorists. Detection of these materials is particularly difficult due to the inherent low-count emissions produced. These low-count emissions result when sources are shielded to disguise their existence or, when being transported, are in relative motion with respect to the sensors. Radionuclide identification from low-count gamma ray emissions is a critical capability that is very difficult to achieve, moreover, this methodology must cope with background noise, finite detector resolution, and the heterogeneous media along transport paths between the sources and detectors. Detection/classification/estimation, therefore, becomes a question of increasing signal-to-noise ratio (*SNR*) in this case, since low-count emissions become buried in the background and Compton scattering noise, rendering a meaningful and timely detection highly improbable [1]-[2].

One of the major challenges is to develop techniques that can provide a timely solution. The basic problem we discuss is the detection and classification of radioactive contraband from highly uncertain (noisy) low-count, radionuclide measurements using a statistical approach based on Bayesian inference and physics-based signal processing. In this paper we develop a Bayesian statistical approach to solve the radiaation detection problem. The usual model-based approach [3] is limited because of two major reasons: (1) the physics models employed do not necessarily capture the true essence of the problem; and (2) the usual statistical machinery to solve such a problem is limited in scope. That is, the contemporary approach is to use linearized approximations to the nonlinear processors (extended and unscented Kalman filters) that imply underlying Gaussian probabilistic assumptions [3]-[5]. Unfortunately the nuclear physics dominating this problem is not characterized as such by unimodal (one peak) distributions, but rather by a multimodal (multiple peaks) representation. We develop physics-based statistical models that capture the essence of this important radiation detection problem and incorporate them into a sequential Bayesian processor which is especially useful when only low count data is available and a rapid detection is required. In general, the model-based approach to signal processing incorporates information about the process (γ-ray emissions), measurement system (semiconductor detectors) and uncertainty or noise (background, random noise, amplitude fluctuations, time jitter, etc.) in the form of mathematical models to develop a model-based processor (*MBP*) [3] capable of enhancing or equivalently extracting signals from highly uncertain environments [2].

Some work has been accomplished on this problem ([5]-[11]), but unfortunately the physics models incorporated into the processor do not capture the true essence of the problem especially from a signal processing perspective. The proposed solutions are based on enhancing the output γ-ray spectrum (energy histogram) by attempting to remove background interference and noise while enhancing the spectral (energy) lines to detect the corresponding radionuclide. The identification of radionuclide sources from their γ-ray emission signatures is a well-established discipline using spectroscopic techniques and algorithms [2]. Unfortunately, these techniques fail on low-count measurement data.

Our approach differs in that it models the source radionuclides by decomposing them uniquely as a superposition (union) of monoenergetic sources that are then smeared and distorted as they are transported through the usual path to the detector for measurement and counting as illustrated in Fig. 1. The measured data consists of a low energy count, impulsive-like, time series measurements (energy vs time) in the form of an *event mode sequence* (*EMS*) obtained from pulse shaping circuitry [2]. The problems of interest are then defined in terms of this unique, orthogonal representation in which solutions based on extracting this characterization from uncertain detector measurements can be postulated.

In Sec. II we develop the physics-based signal processing models employed in the subsequent Bayesian constructs. Here we start with the monoenergetic representation and then incorporate more of the instrumentation and noise into the measurement model. Based on this representation we discuss the overall probabilistic design in Sec. III illustrating how it evolves naturally from the underlying source physics. In Sec. IV we investigate signal processing solutions to the processing

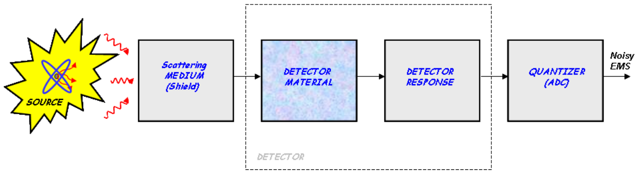

Fig. 1. Gamma-ray evolution and measurement: Radionuclide source (*EMS*), medium transport (physics), detector material interaction, detector temporal response (pre-amplification/pulse shaping) and ADC conversion with quantization noise.

problem as well as develop a sequential detection paradigm for local detection. In Sec. V we develop the overall classification scheme and demonstrate its performance on experimental data. The results of applying the processor to controlled experimental data shows the capability of the sequential Bayesian processor to perform in a reasonable manner. We summarize our results in the final section.

II. PHYSICS-BASED PROCESSING MODELS

The unique characterization of an unstable radionuclide based on its electromagnetic emissions has been an intense area of research and development for well over 50 years [1]-[2]. It is well-known that a particular radionuclide can be uniquely characterized by two basic parameters: its *energy* amplitude levels emitted in the form of photons or gamma-rays (γ-rays) and its radioactive *decay rate* which is directly related to its *arrival time* [2]. Knowledge of one or both of these parameters provides a unique representation of a radionuclide. Mathematically, we define the pair, $[\{\epsilon_m\}, \{\lambda_m\}]$, as the respective energy level (MeV) and decay rate (probability of disintegration/nuclei/sec) of the m^{th}-component of the elemental radionuclide. Although both of these parameters are used to uniquely characterize a radionuclide, only one is actually necessary—unless there is uncertainty in extracting the parameter.

Gamma-ray spectrometry is a methodology to identify radionuclides by estimating the energy (probability) distribution or spectrum and creating a histogram of measured arrival data at various levels (count vs. binned energy) [2]. It essentially decomposes the γ-ray emissions into energy bins discarding the temporal information. As mentioned previously, the role of the γ-ray spectrum is analogous to the role of the Fourier spectrum for identifying sinusoidal spectral lines in noise, a particular radionuclide can be characterized by its inherent "energy spectral lines" in the spectrum. These sharp lines are used to identify the corresponding energy bin detecting the presence of a particular component of the radionuclide. In the ideal case, the spectrum consists only of lines or spikes located at the correct bins of each constituent energy, ϵ_m, uniquely characterizing the radionuclide. A search of the spectrum for the strong presence of these lines is used for identification. The lines are easily identified when the photon interacts with the atoms of the detector material to produce charge directly proportional to its energy. This interaction is called a "photo-peak" which unfortunately occurs only 10% (or less) of the time. Most photons collide with material atoms and are scattered losing energy in the exchange and in a sense "losing its identity," since it is no longer counted in the correct energy bin complicating the spectrum even further.

The key issue in our approach is developing reasonable statistical models of both emission and measurement processes that can effectively be used in the Bayesian framework. These stochastic models of the physical process must incorporate the loss of information resulting from the absorption of energy between an ideal source and the detector. The underlying probability distributions describe the physics of the radiation transport between the source and the detector.

Semiconductor (high purity germanium or sodium iodide) energy detectors are designed to measure the γ-ray energy from the electron current induced by the energy deposition of the incoming photons in the detector material. A typical detector is plagued with a variety of extraneous measurement uncertainties that create inaccuracy and spreading of the measured current impulse (and therefore γ-ray energy). The source radionuclide can be represented by its constituents in terms of monoenergetic (constant energy amplitude) components and arrival times as $\xi(\epsilon_m, \tau_m)$. Since this representation of the source radionuclide contains the constituent energy amplitude levels and timing, then all of the information is completely captured by the sets, $[\{\epsilon_m\}, \{\tau_m\}]$, $m = 1, \cdots, M_\epsilon$. The source arrivals can be used to extract the corresponding set of decay constants, $\{\lambda_m\}$ which are related [2]. Thus, from the detector measurement of the individual photon arrivals or equivalently the entire *EMS*, a particular radionuclide can be uniquely characterized. The constituent energy amplitude levels, $\{\epsilon_m\}$ and arrival times, $\{\tau_m\}$, extracted from the *EMS*.

A. Event Mode Sequence

Next we develop a more detailed mathematical representation of the event mode sequence in terms of its monoenergetic decomposition. From this decomposition, we then develop the basic signal processing model in terms of the random processes that govern its evolution.

Define $\xi(n; \epsilon_m, \tau_m)$ as the component of an *EMS* sequence as the n^{th}-arrival from the m^{th}-monoenergetic source of *energy level* (amplitude), $\epsilon_m(n)$ and *arrival time*, $\tau_m(n)$ with associated *decay rate*, $\lambda_m(n)$ —as a single photon impulse sample, that is, $\xi(n; \epsilon_m, \tau_m) = \epsilon_m(n)\delta(t - \tau_m(n))$ and source rate $\lambda_m(n)$.

The ideal *EMS* is composed of sets of energy-arrival sample pairs, $\{\epsilon_m(n), \tau_m(n)\}$. We could visualize this energy exchange as a photon depositing its energy in the detector material and the pair of unique energy-arrival parameters being extracted by the measurement system.

In order to define the entire emission sequence over a specified time interval, $[t_o, T)$, we introduce the set notation, $\tilde{\tau}_m := \{\ \tau_m(1) \ \cdots \ \tau_m(N_\epsilon(m))\ \}$ at the n^{th}-arrival with $N_\epsilon(m)$ the total number of *counts* for the m^{th}-source in the interval. Therefore, $\xi(n; \epsilon_m, \tilde{\tau}_m)$ results in a unequally-spaced impulse train. The *interarrival* time is defined by $\triangle\tau_m(n) = \tau_m(n) - \tau_m(n-1)$ for $\triangle\tau_m(0) = t_o$ with the corresponding set definition (above) of $\triangle\tilde{\tau}_m(n)$. The *monoenergetic source representation* of a radionuclide source characterized by its unique set of energy/interarrival pairs, $\{\epsilon_m, \triangle\tau_m\}$ (or equivalently as its energy/decay rate pairs, $\{\epsilon_m, \lambda_m\}$) is given by

$$\xi(n; \epsilon_m, \triangle\tilde{\tau}_m) = \sum_{n=1}^{N_\epsilon(m)} \xi(n; \epsilon_m(n), \triangle\tau_m(n)) = \sum_{n=1}^{N_\epsilon(m)} \epsilon_m(n)\delta(t - \triangle\tau_m(n)) \text{ at rate } \lambda_m(n) \quad (1)$$

for t_o known. Let us extend this *EMS* model from a single monoenergetic representation to incorporate a set of M_ϵ-monoenergetic sources that compose a complete source radionuclide. Suppose we have a radionuclide source whose *EMS* is decomposed into its M_ϵ-monoenergetic source components, $\xi(n; \epsilon, \triangle\tilde{\tau})$. From the composition of the *EMS* we know that $\xi(n; \epsilon, \triangle\tilde{\tau}) = \cup_{m=1}^{M_\epsilon} \xi(n; \epsilon_m, \triangle\tilde{\tau}_m) \Leftrightarrow \sum_{m=1}^{M_\epsilon} \xi(n; \epsilon_m, \triangle\tilde{\tau}_m)$; where the last equivalence results from the pragmatic assumption that it is highly *improbable* that any two arrivals will overlap. Thus, it follows that a complete radionuclide can be represented in terms of its monoenergetic decomposition, that is, the *EMS* is:

$$\mathcal{R}_\eta(n; \underline{\epsilon}, \triangle\underline{\tau}) = \sum_{m=1}^{M_\epsilon} \sum_{n=1}^{N_\epsilon(m)} \xi(n; \epsilon_m(n), \triangle\tau_m(n)) = \sum_{m=1}^{M_\epsilon} \sum_{n=1}^{N_\epsilon(m)} \epsilon_m(n)\delta(t - \triangle\tau_m(n)) \quad (2)$$

where $\mathcal{R}_\eta(n; \underline{\epsilon}, \triangle\underline{\tau})$ is the composite *EMS* of the radionuclide, M_ϵ is the number of monoenergetic source components in the composite *EMS*, $N_\epsilon(m)$ is the number (counts) of arrivals from the *mth*-monoenergetic source component in the time-interval, $[t_o, T)$, $\epsilon_m(n)$ is the *nth*-arrival of γ-ray energy (amplitude) level of the *mth*-monoenergetic component in the time-interval of the composite *EMS*, $\triangle\tau_m(n)$ is the *nth* interarrival time of the *mth*-monoenergetic component, in the time interval of the composite *EMS*. This representation can be extended even further to capture a set of radionuclides as well. Thus, this unique physics-based representation provides the basis to develop signal models for subsequent processing.

B. Detector Measurements

The *pulse-mode* of detector (semiconductor) operation, is the most common technique employed in γ-ray detection, since both amplitude and arrivals are measured [2]. Amplitude variations are typically expressed in terms of the differential pulse height (amplitude) distribution which is a direct representation of the uncertainty in measuring the energy level. This distribution is commonly called the *detector response function* [2] and can be modeled in terms of our monoenergetic source amplitude (energy amplitude level). Here the detector response characterizes the energy deposited in the detector material scaled to produce the equivalent charge (current) at the pulse amplifier input electronics.

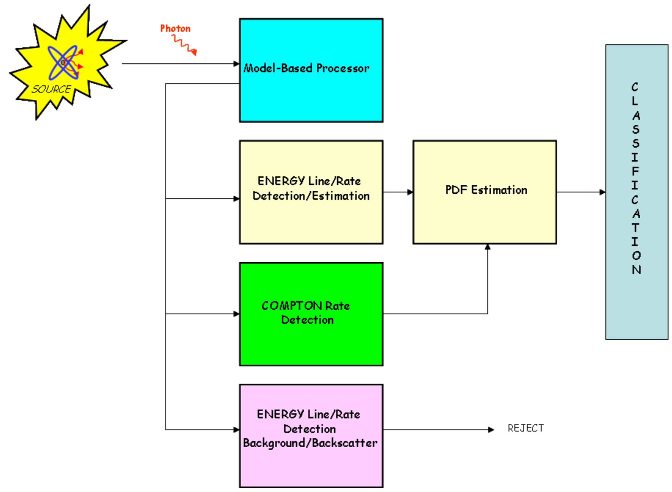

Fig. 2. Bayesian radiation detection: Acquisition, pre-processing (*MBP*), energy/rate discrimination, Compton processing, background and extraneous line rejection, probability density function estimation and classification.

Lumping the material uncertainties into an additive noise process, the measured nth-interarrival of the mth-monoenergetic component can be characterized by

$$p_m(n) = \epsilon_m(n)\delta(t - \triangle\tau_m(n)) + w_{\triangle\tau_m}(n)$$

where the uncertain energy amplitude level is assumed Gaussian, $\epsilon \sim \mathcal{N}(\bar{\epsilon}_m, \sigma^2_{\epsilon_m})$, with inherent uncertainty representing the material charge collection process time "jitter" by the additive zero-mean, Gaussian noise, $w_{\triangle\tau_m} \sim \mathcal{N}(\triangle\bar{\tau}_i, \sigma^2_{w_{\triangle\tau_m}})$. Next we investigate the use of these models in Bayesian processor designs.

III. PHYSICS-BASED RADIONUCLIDE DETECTION

Since all of the measurement data and required parameters evolve from the *EMS*, we are in search of an estimator/detector that enables us to "decide" when a particular target radionuclide is present or not. We show the inherent structure of the processor in Fig. 2. After the single photon is processed by the acquisition system, the extracted parameters are enhanced and passed onto the energy/rate discriminators to "decide" on the photon's status (line/rate, Compton, reject). If acceptable, the probability density function estimates are sequentially updated and provided as input to the radionuclide detector.

We start with estimating the posterior distribution (or its equivalent) from the uncertain data, that is,

$$\Pr(\mathcal{R}_\eta(n; \underline{\epsilon}, \triangle\underline{\tau})|\Xi_n) \quad \Leftrightarrow \quad \Pr(\underline{\epsilon}, \triangle\underline{\tau})|\Xi_n)$$

for $\underline{\epsilon} := \{\epsilon_1(n), \cdots, \epsilon_{M_\epsilon}(n)\}$, the complete set of energy amplitude levels composing $\mathcal{R}_\eta$ along with $\triangle\underline{\tau} := \{\triangle\tau_1(n), \cdots, \triangle\tau_{M_\epsilon}(n)\}$, the corresponding set of interarrival times with $\Xi_n := \{\xi(1), \cdots, \xi(n)\}$, the set of *EMS* measurements including the nth-arrival.

Unfortunately, the basic radionuclide physics is more complicated, since the emission of monoenergetic photons follows a well-defined probability structure, that is, *all* monoenergetic photons are *not* present in the *EMS* during an individual event (single photon arrival) only *one* of the energy amplitude levels is present as dictated by its branching or probability of occurrence (α_i) associated with its inherent structure as specified in its energy decay diagram [2]. Therefore, we model this decay structure by a Markov chain model ([12],[13]) incorporating an *indicator function* defined by:

$$\mathcal{I}_j(m) = \begin{cases} 1 & m = j \\ \\ 0 & m \neq j \end{cases}$$

where $\mathcal{I}_j(m)$ is a random variable such that $\Pr(\mathcal{I}_j(m) = 1|\xi(n;\underline{\epsilon},\underline{\tau}) = \Pr(\mathcal{I}_j(m) = 1|\Xi_n) = \alpha_j$ for α_j the corresponding branching or *probability of occurrence* of the jth-monoenergetic RN component.

Incorporating this additional physics information (α_j) based on the energy level diagrams of various radionuclides [2], we can model the radionuclide by its monoenergetic decomposition embedding the corresponding indicator function, $\mathcal{I}_j(m)$, such that

$$\mathcal{R}_\eta(n;\underline{\epsilon},\triangle\underline{\tau}) = \sum_{m=1}^{M_\epsilon} \xi(n;\epsilon_m,\triangle\tau_m) = \sum_{m=1}^{M_\epsilon}\sum_{n=1}^{N_\epsilon(m)} \mathcal{I}_j(m)\epsilon_m(n)\delta(t-\triangle\tau_m(n)) \qquad (3)$$

and therefore, for the jth-monoenergetic source we have

$$\xi(n;\epsilon_m,\triangle\tau_m)|_{m\to j} = \sum_{n=1}^{N_\epsilon(j)} \epsilon_j(n)\delta(t-\triangle\tau_j(n)) \qquad (4)$$

With this in mind, the required radionuclide posterior distribution can be decomposed in terms of each arrival pair $(\epsilon_j(n),\triangle\tau_j(n))$ along with its associated probability of occurrence, α_j, that is,

$$\Pr\left(\mathcal{R}_\eta(n;\underline{\epsilon},\triangle\underline{\tau})|\Xi_n\right) = \Pr\left(\underline{\epsilon}(n),\triangle\underline{\tau}(n),\mathcal{I}_j(m)|\Xi_n\right) \qquad (5)$$

Applying Bayes' rule we obtain

$$\begin{aligned} &\Pr\left(\mathcal{R}_\eta(n;\underline{\epsilon},\triangle\underline{\tau})|\Xi_n\right) = \Pr\left(\triangle\underline{\tau}(n)|\underline{\epsilon}(n),\mathcal{I}_j(m),\Xi_n\right) \\ \times\; &\Pr\left(\underline{\epsilon}(n)|\mathcal{I}_j(m),\Xi_n\right) \times \Pr\left(\mathcal{I}_j(m)|\Xi_n\right) \qquad (6) \end{aligned}$$

The *posterior radionuclide probability* can be estimated photon-by-photon and therefore evolves to the following processor:

1) *Given* the "truth": $[\{\alpha_m^t\},\{\epsilon_m^t\},\{\triangle\tau_m^t\}]\,; m = 1,\cdots,M_\epsilon$ (from Tables);
2) *Determine* the jth-monoenergetic component with $\Pr(\mathcal{I}_j(m) = 1) = \alpha_j$, *decide* on energy-interarrival pair $(\epsilon_j,\triangle\tau_j)$;
3) *Given* $m = j$ and the data Ξ_n, estimate the *energy amplitude distribution*: $\hat{\Pr}(\epsilon_j(n)|\Xi_n)$;
4) *Given* $\epsilon_j(n)$ and the data Ξ_n, estimate the *interarrival distribution*: $\hat{\Pr}(\triangle\tau_j(n)|\epsilon_j(n),\Xi_n)$;
5) *Update* the radionuclide posterior distribution $\Pr\left(\mathcal{R}_\eta(n;\epsilon_j,\triangle\tau_j)|\Xi_n\right)$ using Eq. 6; and
6) *Decide* if this estimated distribution "matches" the target radionuclide distribution.

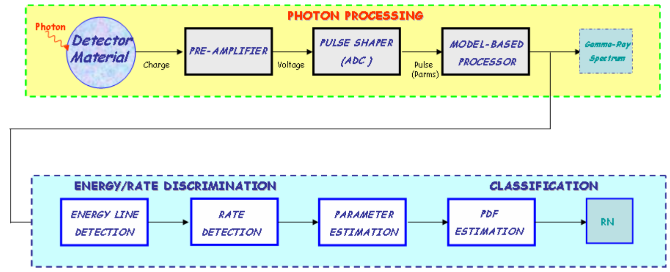

Fig. 3. Bayesian radiation detection channel details: acquisition, pre-processing (*MBP*), energy/rate discrimination and classification.

It is the joint relation of Eq. 6 that motivates the design of the processor. We note first that in this construct the interarrival times are conditioned on the energy amplitude levels and data implying that we *first* extract these amplitudes from the *EMS*. This also leads us to the required posterior based on $\underline{\epsilon}$. Next, using the knowledge of the amplitude, we extract the corresponding interarrival.

A single photon channel processor for energy line/rate detection is shown in Fig. 3 after the acquisition and pre-processing steps are performed along with a pulse-height spectrum (*PHS*) estimate (not required). Simple energy amplitude level and rate detectors are first performed to determine the status (accept or reject) of the processed photon—these discriminators implement the indicator function discussed previously. If acceptable, this photon is used to estimate the required posterior distribution for radionuclide detection.

After the photon is processed by a model-based processor (optional), the distributed detector: (1) discriminates the individual monoenergetic amplitudes identifying one of the parallel channels; (2) discriminates the corresponding rate parameter for that particular channel confirming the monoenergetic source detection from two parameters rather than one amplitude parameter; (3) estimates or enhances the particular amplitude and rate parameters along with the corresponding distributions enabling the estimation of the radionuclide posterior; and (5) detects/classifies the target RN.

To summarize, we are essentially implementing the monoenergetic decomposition using discriminators to decide which threat energy amplitude level/rate channel the photon belongs to or rejecting it completely if no such channel indicates a valid detection. All of the physics information is combined in the decision function thereby by the monoenergetic source parameters, $(\epsilon_m^t,\triangle\tau_m^t,\alpha_m^t)$. This completes the conceptual design of the Bayesian processor for radionuclide detection, next we develop the various components of the processor for implementation.

IV. SEQUENTIAL BAYESIAN DETECTION

In this section, we develop the sequential Bayesian framework and individual components of the processor. To formally pose this problem, we appeal to classical (sequential) detection theory [14]. We are to test the binary hypothesis that the measured *EMS* has evolved from the targeted radionuclide (RN) characterized uniquely from its monoenergetic decomposition of Eq. 3. Therefore, we specify the hypothesis test

$$\begin{aligned}\mathcal{H}_0:\ & \xi(n;\underline{\epsilon},\triangle\underline{\tau}) = \mathcal{R}_\eta(n;\underline{\epsilon},\triangle\underline{\tau}) + \nu(n) \quad \text{[NON-TARGET]}\\ \mathcal{H}_1:\ & \xi(n;\underline{\epsilon},\triangle\underline{\tau}) = \mathcal{R}_\eta(n;\underline{\epsilon}^t,\triangle\underline{\tau}^t) + \nu(n) \quad \text{[TARGET]}\end{aligned}$$

where $\mathcal{R}_\eta(n;\underline{\epsilon},\triangle\underline{\tau})$ is a random composite *EMS* contaminated with zero-mean, Gaussian measurement (instrumentation) noise, $\nu \sim \mathcal{N}(0,\sigma_\nu^2)$ and

$$\mathcal{R}_\eta(n;\underline{\epsilon},\triangle\underline{\tau}) = \sum_{m=1}^{M_\epsilon}\sum_{n=1}^{N_\epsilon(m)} \mathcal{I}_j(m)\epsilon_m(n)\delta\left(t-\triangle\tau_m(n)\right) \quad (7)$$

for $\epsilon_m \sim \mathcal{N}(\overline{\epsilon}_m,\sigma_{\epsilon_m}^2)$ and $\triangle\tau_m \sim \mathcal{E}(\lambda_{\triangle\tau_m}\triangle\tau_m(n))$.

The optimal solution to this binary decision problem is based on applying the *Neyman-Pearson theorem* leading to the sequential likelihood ratio [14] given by the recursion or equivalently sequential likelihood ratio for the *nth* arrival as

$$\mathcal{L}[\Xi_n] = \mathcal{L}[\Xi_{n-1}] \times \frac{\Pr(\xi(n;\underline{\epsilon},\triangle\underline{\tau})|\Xi_{n-1},\mathcal{H}_1)}{\Pr(\xi(n;\underline{\epsilon},\triangle\underline{\tau})|\Xi_{n-1},\mathcal{H}_0)} \quad (8)$$

Since the distributions under investigation are members of the exponential family [12], then taking logarithms simplifies the computations. We define $\Lambda[\Xi_n] := \ln\mathcal{L}[\Xi_n]$ to obtain the *sequential log-likelihood*

$$\begin{aligned}\Lambda[\Xi_n] &= \Lambda[\Xi_{n-1}] + \ln\Pr(\xi(n;\underline{\epsilon},\triangle\underline{\tau})|\Xi_{n-1},\mathcal{H}_1)\\ &- \ln\Pr(\xi(n;\underline{\epsilon},\triangle\underline{\tau})|\Xi_{n-1},\mathcal{H}_0) \quad (9)\end{aligned}$$

and therefore, the Wald *sequential probability-ratio test* becomes

$$\begin{array}{cccc} & \Lambda[\Xi_n] & \geq \ln\mathcal{T}_1(n) & \text{Accept}\quad \mathcal{H}_1\\ \ln\mathcal{T}_0(n) & \leq \Lambda[\Xi_n] & \leq \ln\mathcal{T}_1(n) & \text{Continue}\\ & \Lambda[\Xi_n] & \leq \ln\mathcal{T}_0(n) & \text{Accept}\quad \mathcal{H}_0\end{array} \quad (10)$$

where the thresholds are specified in terms of the false alarm (P_{FA}) and miss (P_M) probabilities as

$$\mathcal{T}_0(n) = \frac{P_M(n)}{P_{FA}(n)} \qquad \mathcal{T}_1(n) = \frac{1-P_M(n)}{P_{FA}(n)}$$

So we see that at each photon arrival (at time n), we *sequentially update* the likelihood and thresholds to perform the detection — "photon-by-photon". To implement the sequential detector, we must specify the required distributions; therefore, we have

$$\begin{aligned}&\Pr(\xi(n;\underline{\epsilon},\triangle\underline{\tau})|\Xi_{n-1},\mathcal{H}_\ell) =\\ &\Pr(\mathcal{R}_\eta(n;\underline{\epsilon},\triangle\underline{\tau},\mathcal{I}_j(m)|\Xi_{n-1},\mathcal{H}_\ell) + \Pr(\nu(n)|\Xi_{n-1},\mathcal{H}_\ell)\end{aligned} \quad (11)$$

for the hypotheses specified by $\mathcal{H}_\ell;\ \ell = 0,1$.

Using the monoenergetic radionuclide model, we obtain

$$\begin{aligned}&\Pr(\xi(n;\underline{\epsilon},\triangle\underline{\tau})|\Xi_{n-1},\mathcal{H}_\ell) =\\ &\Pr(\underline{\epsilon}(n),\triangle\underline{\tau}(n),\mathcal{I}_j(m)|\Xi_{n-1},\mathcal{H}_\ell) + \Pr(\nu(n)|\Xi_{n-1},\mathcal{H}_\ell)\end{aligned} \quad (12)$$

Applying Bayes' rule, we obtain the decomposition (as before)

$$\begin{aligned}&\Pr(\xi(n;\underline{\epsilon},\triangle\underline{\tau})|\Xi_{n-1},\mathcal{H}_\ell) =\\ &\Pr(\triangle\underline{\tau}(n)|\underline{\epsilon}(n),\mathcal{I}_j(m),\Xi_{n-1},\mathcal{H}_\ell) \times \Pr(\underline{\epsilon}(n)|\mathcal{I}_j(m),\Xi_{n-1},\mathcal{H}_\ell)\\ &\times\Pr(\mathcal{I}_j(m)|\Xi_{n-1},\mathcal{H}_\ell) + \Pr(\nu(n)|\Xi_{n-1},\mathcal{H}_\ell)\end{aligned} \quad (13)$$

Decomposing the parameter vectors using the fact that each arrival has "no memory" and applying the chain rule of probability, we obtain

$$\begin{aligned}\Pr(\triangle\underline{\tau}(n) &\ |\ \underline{\epsilon}(n),\mathcal{I}_j(m),\Xi_{n-1},\mathcal{H}_\ell)\\ = \prod_{m=1}^{M_\epsilon}\Pr(\triangle\tau_m(n) &\ |\ \epsilon_m(n),\mathcal{I}_j(m),\Xi_{n-1},\mathcal{H}_\ell)\\ \Pr(\underline{\epsilon}(n),\mathcal{I}_j(m) &\ |\ \Xi_{n-1},\mathcal{H}_\ell)\\ = \prod_{m=1}^{M_\epsilon}\Pr(\epsilon_m(n) &\ |\ \mathcal{I}_j(m),\Xi_{n-1},\mathcal{H}_\ell)\\ \times &\ \ \Pr(\mathcal{I}_j(m)|\Xi_{n-1},\mathcal{H}_\ell)\end{aligned} \quad (14)$$

and therefore, we have

$$\begin{aligned}&\Pr(\xi(n;\underline{\epsilon},\triangle\underline{\tau})|\Xi_{n-1},\mathcal{H}_\ell) =\\ &\prod_{m=1}^{M_\epsilon}\Pr(\triangle\tau_m(n)|\epsilon_m(n),\mathcal{I}_j(m),\Xi_{n-1},\mathcal{H}_\ell)\times\\ &\Pr(\epsilon_m(n)|\mathcal{I}_j(m),\Xi_{n-1},\mathcal{H}_\ell)\times\Pr(\mathcal{I}_j(m)|\Xi_{n-1},\mathcal{H}_\ell)\\ +\ &\Pr(\nu(n)|\Xi_{n-1},\mathcal{H}_\ell);\ell=0,1\end{aligned} \quad (15)$$

Substituting these distributions into Eq. 9 the *sequential log-likelihood ratio* detector is

$$\begin{aligned}&\Lambda[\Xi_n] = \Lambda[\Xi_{n-1}] +\\ &\sum_{m=1}^{M_\epsilon}\ln\Big(\Pr(\triangle\tau_m^t(n)|\epsilon_m^t(n),\mathcal{I}_j^t(m),\Xi_{n-1},\mathcal{H}_1)\times\\ &\Pr(\epsilon_m^t(n),\mathcal{I}_j^t(m)|\Xi_{n-1},\mathcal{H}_1) + \Pr(\nu(n)|\Xi_{n-1},\mathcal{H}_1)\Big)\\ &-\sum_{m=1}^{M_\epsilon}\ln\Big(\Pr(\triangle\tau_m(n)|\epsilon_m(n),\mathcal{I}_j(m),\Xi_{n-1},\mathcal{H}_0)\times\\ &\Pr(\epsilon_m(n),\mathcal{I}_j(m)|\Xi_{n-1},\mathcal{H}_0) + \Pr(\nu(n)|\Xi_{n-1},\mathcal{H}_0)\Big)\end{aligned} \quad (16)$$

where

$$\begin{aligned}&\Pr(\epsilon_m(n),\mathcal{I}_j(m)|\Xi_{n-1},\mathcal{H}_\ell) =\\ &\Pr(\epsilon_m(n)|\mathcal{I}_j(m),\Xi_{n-1},\mathcal{H}_\ell)\times\Pr(\mathcal{I}_j(m)|\Xi_{n-1},\mathcal{H}_\ell)\end{aligned}$$

giving us the general form for our problem[1]. Note that this formulation provides us with a channel-by-channel (photon-by-photon) processor, since the *mth* terms are available at the output of each channel

[1]Note that this decision function not only incorporates the energy amplitude level (ϵ_m) and interarrival time-tags ($\triangle\tau_m$) for each constituent monoenergetic source composing the target radionuclide, but also the probability of occurrence or branching probability (α_m) which acts as a weighting function in the overall superposition enabling all of the energy lines to be combined.

Let us further assume that the instrumentation noise ($\nu(n)$) is *small* relative to the inherent parametric uncertainties and ignore it, then the log-likelihood ratio simplifies to

$$\begin{aligned}
&\Lambda[\Xi_n] = \Lambda[\Xi_{n-1}] + \\
&\sum_{m=1}^{M_\epsilon} \ln \Pr(\triangle\tau_m^t(n)|\epsilon_m^t(n), \mathcal{I}_j^t(m), \Xi_{n-1}, \mathcal{H}_1) + \\
&\ln \Pr(\epsilon_m^t(n), \mathcal{I}_j^t(m)|\Xi_{n-1}, \mathcal{H}_1) - \\
&\sum_{m=1}^{M_\epsilon} \ln \Pr(\triangle\tau_m(n)|\epsilon_m(n), \mathcal{I}_j(m), \Xi_{n-1}, \mathcal{H}_0) + \\
&\ln \Pr(\epsilon_m(n), \mathcal{I}_j(m)|\Xi_{n-1}, \mathcal{H}_0)
\end{aligned} \tag{17}$$

where we have applied the log transform and Bayes' rule above completing the decision function.

A. Sequential Radiation Detection

In this section we develop the statistical models (ignoring the measurement noise) to implement the likelihood-ratio detector. Since each individual RN is uniquely specified (statistically) by its parameter set, $\{\underline{\epsilon}, \triangle\underline{\tau}, \underline{\alpha}\}$, we assume that α is known for each target (from tables). Using the energy amplitude level distribution and its decomposition of Eq. 14 the jth-monoenergetic source component selected by the indicator function, $\mathcal{I}_j(m)$ is therefore

$$\Pr(\epsilon_j(n), \mathcal{I}_j(m)|\Xi_{n-1}, \mathcal{H}_\ell) = \alpha_j \Pr(\epsilon_j(n)|\Xi_{n-1}, \mathcal{H}_\ell) \tag{18}$$

where we have applied $\Pr(\mathcal{I}_j(m) = 1|\Xi_{n-1}) = \alpha_j$.

Each energy amplitude component is assumed Gaussian with corresponding distribution

$$\begin{aligned}
\Pr(\epsilon_m(n) \quad &| \quad \mathcal{I}_j(m), \Xi_{n-1}, \mathcal{H}_\ell) \sim \mathcal{N}(\overline{\epsilon}_j(n), \sigma_{\epsilon_j}^2) \\
&= \quad \frac{1}{\sqrt{2\pi}\sigma_{\epsilon_j}} \exp\left\{-\frac{(\epsilon_j(n) - \overline{\epsilon}_j(n))^2}{2\sigma_{\epsilon_j}^2}\right\}
\end{aligned} \tag{19}$$

Finally, the interarrival times, $\triangle\underline{\tau}$, are assumed *conditionally independent* of both $\underline{\epsilon}$ and $\mathcal{I}_j(m)$ and exponentially distributed such that

$$\begin{aligned}
\Pr(\triangle\underline{\tau}(n) \quad &| \quad \mathcal{I}_j(m), \Xi_{n-1}, \mathcal{H}_\ell) = \\
&\prod_{m=1}^{M_\epsilon} \Pr(\triangle\tau_m(n)|\mathcal{I}_j(m), \Xi_{n-1}, \mathcal{H}_\ell) \\
&= \quad \prod_{m=1}^{M_\epsilon} \lambda_{\triangle\tau_m} \exp\{-\alpha_m\lambda_{\triangle\tau_m}\triangle\tau_m(n)\}
\end{aligned} \tag{20}$$

with α_m the probability of occurrence and for the rate $\lambda_{\triangle\tau_m} = 1/\overline{\triangle\tau_m}$, that is, the reciprocal of the mean interarrival time. For the jth-monoenergetic source component, we have

$$\begin{aligned}
\Pr(\triangle\underline{\tau}(n) \quad &| \quad \mathcal{I}_j(m), \Xi_{n-1}, \mathcal{H}_\ell) \sim \mathcal{E}(\alpha_j\lambda_{\triangle\tau_j}\triangle\tau_j(n)) \\
&= \quad \lambda_{\triangle\tau_j} \exp\{-\alpha_j\lambda_{\triangle\tau_j}\triangle\tau_j(n)\}
\end{aligned} \tag{21}$$

With these distribution models in hand, we can now construct the sequential detection algorithm as

$$\begin{aligned}
&\Pr(\xi(n; \underline{\epsilon}, \triangle\underline{\tau})|\mathcal{I}_j(m), \Xi_{n-1}, \mathcal{H}_\ell) \\
&= \prod_{m=1}^{M_\epsilon} \lambda_{\triangle\tau_m} \exp\{-\alpha_m\lambda_{\triangle\tau_m}\triangle\tau_m(n)\} \\
&\times \frac{\alpha_m}{\sqrt{2\pi}\sigma_{\epsilon_m}} \exp\left\{-\frac{(\epsilon_m(n) - \overline{\epsilon}_m(n))^2}{2\sigma_{\epsilon_m}^2}\right\} \\
+ \quad &\frac{1}{\sqrt{2\pi}\sigma_\nu} \exp\left\{-\frac{\nu^2(n)}{2\sigma_\nu^2}\right\}
\end{aligned} \tag{22}$$

which leads to the *sequential log-likelihood ratio* detection processor of Eq. 17 (assuming the instrumentation noise is small) and using the "true" parameters $\{\epsilon_m^t, \triangle\tau_m^t, \alpha_m^t\}$ for $\mathcal{H}_1$ as

$$\begin{aligned}
&\Lambda[\Xi_n] = \Lambda[\Xi_{n-1}] + \sum_{m=1}^{M_\epsilon} \ln\left(\frac{\alpha_m^t\lambda_{\triangle\tau_m}^t}{\sqrt{2\pi}\sigma_{\epsilon_m^t}}\right) \\
&-\ln\left(\frac{\alpha_m\lambda_{\triangle\tau_m}}{\sqrt{2\pi}\sigma_{\epsilon_m}}\right) + \left(\alpha_m\lambda_{\triangle\tau_m} - \alpha_m^t\lambda_{\triangle\tau_m}^t\right)\triangle\tau_m(n) \\
&+\frac{1}{2}\left(\frac{\epsilon_m(n) - \overline{\epsilon}_m(n)}{\sigma_{\epsilon_m}}\right)^2 - \frac{1}{2}\left(\frac{\epsilon_m(n) - \epsilon_m^t(n)}{\sigma_{\epsilon_m^t}}\right)^2
\end{aligned} \tag{23}$$

This completes the structure of the sequential Bayesian radiation detector, we will discuss the actual photon-by-photon implementation of this processor in a subsequent section. Again note the incorporation of all of the physics information available ($\epsilon_m, \triangle\tau_m, \alpha_m$) the decision function (see previous footnote).

B. Sequential Bayesian Parameter Estimation

In order to implement this radionuclide detection scheme, we must estimate the underlying parameter (amplitude and interarrival time) distributions. Investigating the monoenergetic *EMS* decomposition of a radionuclide $\mathcal{R}_\eta$ with M_ϵ monoenergetic source components and $N_e(m)$ counts in the total interval of count length N, we can define an overall parameter vector by

$$\begin{aligned}
&\Theta := [\underline{\epsilon} \ \mid \ \underline{\tau} \ \mid \ \underline{\alpha}] = \\
&[\epsilon_1 \ \cdots \ \epsilon_{M_\epsilon} \ \mid \ \triangle\tau_1 \ \cdots \ \triangle\tau_{M_\epsilon} \ \mid \ \alpha_1 \ \cdots \ \alpha_{M_\epsilon}]
\end{aligned}$$

for $\Theta \in \mathcal{R}^{2M_\epsilon \times 1}$ requiring $3M_\epsilon$ parameters to specify the unknown radionuclide. The number of arrivals counted in the interval N is $N_\epsilon := [N_\epsilon(1) \quad \cdots \quad N_\epsilon(M_\epsilon)]$ such that $N = \sum_{m=1}^{M_\epsilon} N_\epsilon(m)$, as before.

We assume that the energy amplitudes can be characterized by a random walk model

$$\underline{\epsilon}(n) = \underline{\epsilon}(n-1) + \underline{w}_\epsilon(n-1) \tag{24}$$

for $\underline{\epsilon}, \underline{w} \in \mathcal{R}^{2M_\epsilon \times 1}$ and $\underline{\epsilon} \sim \mathcal{N}(\overline{\epsilon}, R_{\overline{\epsilon\epsilon}})$; $\underline{w}_\epsilon \sim \mathcal{N}(0, R_{w_\epsilon w_\epsilon})$. The measurement instrument measures both photon energy amplitude and interarrival time from the *EMS*; therefore, it provides the vector measurement

$$\underline{\xi}(n) := [\ \xi_\epsilon(n) \ \mid \ \xi_{\triangle\tau}(n)\ ]' \tag{25}$$

We model the energy amplitude component as the level contaminated with zero-mean, Gaussian instrumentation noise such that

$$\xi_\epsilon(n) = \underline{c}'\underline{\epsilon}(n) + v_\epsilon(n) = \epsilon_m(n) + v_\epsilon(n) \tag{26}$$

since the scalar measurement is photon-by-photon with $v_\epsilon \sim \mathcal{N}(0, R_{v_\epsilon v_\epsilon})$. The measurement system vector $\underline{c}'$ is a $1 \times M_\epsilon$, unit row vector, that is, $\underline{c}' = \underline{e}'_m$ with a one in the *mth* column. Thus, our final photon energy amplitude level model is given by a Gauss-Markov representation

$$\begin{aligned} \underline{\epsilon}(n) &= \underline{\epsilon}(n-1) + \underline{w}_\epsilon(n-1) \\ \xi_\epsilon(n) &= \underline{c}'\underline{\epsilon}(n) + v_\epsilon(n) \end{aligned} \tag{27}$$

with noise sources $\underline{w}_\epsilon$ and $\underline{v}_\epsilon$ characterized by zero-mean, multivariate Gaussian distribution with covariance matrices, $R_{w_\epsilon w_\epsilon}$ and $R_{v_\epsilon v_\epsilon}$, respectively and the initial states the true mean values characterizing the target RN, $\underline{\epsilon}(0) \sim \mathcal{N}(\overline{\epsilon}_o, R_{\overline{\epsilon}_o \overline{\epsilon}_o})$.

Since we first *discriminate* the energy amplitude level to determine which channel to process it, the actual implementation requires only a scalar algorithm for the *mth*-monoenergetic line, that is, the monoenergetic line estimator is based on the Markovian representation as

$$\begin{aligned} \epsilon_m(n) &= \epsilon_m(n-1) + w_{\epsilon_m}(n-1) \\ \xi_\epsilon(n) &= \epsilon_m(n) + v_\epsilon(n) \end{aligned} \tag{28}$$

with $\epsilon_m(0) \sim \mathcal{N}(\overline{\epsilon}_m, R_{\overline{\epsilon}_m \overline{\epsilon}_m})$ and $w_{\epsilon_m} \sim \mathcal{N}(0, R_{w_{\epsilon_m} w_{\epsilon_m}})$;$v_\epsilon \sim \mathcal{N}(0, R_{v_\epsilon v_\epsilon})$. Thus, photon-by-photon processing leads to a scalar channel-by-channel implementation.

Since these characterizations are linear Gauss-Markov models [3], we know that the optimal Bayesian processor is the linear Kalman filter with posterior distribution given by

$$\Pr(\epsilon_m(n)|\Xi_n) \sim \mathcal{N}(\hat{\epsilon}_m(n|n), \tilde{\sigma}^2_{\epsilon_m}(n|n))$$

with conditional mean and variance specified by

$$\begin{aligned} \hat{\epsilon}_m(n|n) &= \hat{\epsilon}_m(n|n-1) + K_{\epsilon_m}(n) e_m(n) \\ e_m(n) &= \epsilon_m(n) - \hat{\epsilon}_m(n|n-1) \\ K_{\epsilon_m}(n) &= \tilde{\sigma}^2_{\epsilon_m}(n|n)/\sigma^2_{e_m}(n) \end{aligned} \tag{29}$$

where $\hat{\epsilon}_m(n|n)$ is the conditional mean estimate of the *mth*-energy amplitude level at arrival time n based on all of the data up to n; $\tilde{\sigma}^2_{\epsilon_m}$ is the corresponding error covariance, $\text{cov}(\epsilon_m(n) - \hat{\epsilon}_m(n|n))$; $e_m(n)$ is the innovations sequence with covariance, $\sigma^2_{e_m}(n) = \text{cov}(e_m(n))$ and K_{ϵ_m} is the weight or gain matrix [3]. Next we consider the interarrival processor.

From the statistics of the *EMS* process, we know that the interarrival times are exponentially distributed with parameter $\lambda_{\triangle\tau}$ such that $\triangle\tau(n) \sim \mathcal{E}(\lambda_{\triangle\tau}\triangle\tau(n)) = \lambda_{\triangle\tau}\exp(-\lambda_{\triangle\tau} \times \triangle\tau(n))$. Our process model for the interarrival time is just an exponential random variable, while the underlying measurement model is this variable contaminated with exponential measurement (instrumentation) noise given by

$$\begin{aligned} &\triangle\tau_m(n) = w_{\triangle\tau_m}(n) \\ &\xi_{\triangle\tau}(n) = \triangle\tau_m(n) + v_{\triangle\tau_m}(n) \end{aligned} \tag{30}$$

for $w_{\triangle\tau_m} \sim \mathcal{E}(\alpha_m \lambda_{\triangle\tau_m} \triangle\tau_m(n))$ and $v_{\triangle\tau_m} \sim \mathcal{E}(\lambda_\nu v_{\triangle\tau_m}(n))$. The corresponding likelihood for this problem is obtained using the measurement model and the transformation of random variable rules [12] to give

$$\Pr(\xi_{\triangle\tau}(n)|\triangle\tau(n)) = \lambda_\nu e^{-\lambda_\nu \ (\xi_{\triangle\tau}(n) - \triangle\tau(n))} \tag{31}$$

We estimate the posterior distribution using a sequential Monte Carlo approach and construct a *bootstrap particle filter* [4] using the following steps:

- Initialize: $\triangle\tau_m(0) \sim \mathcal{E}(\overline{\triangle}\tau_m(0))$, $w_{\triangle\tau_m} \sim \mathcal{E}(\alpha_m \lambda_{\triangle\tau_m} \triangle\tau_m(n))$, $W_i(0) = 1/N_p; i = 1, \cdots, N_p$;
- State Transition: $\triangle\tau_{m_i}(n) = w_{\triangle\tau_{m_i}}(n)$ for $w_{m_i} \sim \Pr(w_{m_i}(n))$;
- Log-Likelihood: $\ln \mathcal{C}(\xi_{\triangle\tau_m}(n)|\triangle\tau_{m_i}(n)) = \ln\lambda_\nu - \lambda_\nu \times (\xi_{\triangle\tau}(n) - \triangle\tau(n))$;
- Weights: $W_i(n) = W_i(n-1) \times \mathcal{C}(\xi_{\triangle\tau_m}(n)|\triangle\tau_{m_i}(n))$;
- Normalize: $\mathcal{W}_i(n) = \frac{W_i(n)}{\sum_{i=1}^{N_p} W_i(n)}$;
- Resample: $\triangle\hat{\tau}_{m_i}(n) \Rightarrow \triangle\tau_{m_i}(n)$;
- Posterior: $\hat{\Pr}(\triangle\tau_m(n)|\Xi_n) = \sum_{i=1}^{N_p} \mathcal{W}_i(n)\delta(\xi_{\triangle\tau_m}(n) - \xi_{\triangle\tau_{m_i}}(n))$; and
- MAP Estimate: $\triangle\hat{\tau}(n|n) = \arg\max \hat{\Pr}(\triangle\tau_m(n)|\Xi_n)$.

So we see that the sequential likelihood radionuclide detector evolves from estimating the posterior distributions that require parameter estimates of energy "line" amplitude, rate (interarrival times) and occurrence probabilities for implementation. We used a Rao-Blackwellization [16] approach by partitioning the state vector into the amplitude and interarrival estimators and applying a linear Kalman filter for the Gaussian distributed amplitude and a particle filter for the exponentially distributed interarrival times (rate)—channel-by-channel.

C. Sequential Bayesian Processor Implementation

In this section we discuss the implementation of the processor for the radionuclide detection processor following the design structure developed in Sec. 3. First, we investigate the individual channel processor illustrated in Fig. 3 one for each energy amplitude/rate composing the target radionuclide.

1) Energy Amplitude Level/Interarrival (Rate) Discriminator: We apply an energy amplitude discriminator to "decide" on which channel the photon should be processed and followed by a rate discriminator using the interarrival "time tag". The discriminator used implied hypothesis testing by constructing a confidence interval about the means of the respective parameters. The *energy amplitude level* discriminator performs the following confidence interval test to accept or reject the photon:

$$[\epsilon_{tru} - \kappa_\alpha \sigma_\xi \leq \epsilon_m(n) \leq \epsilon_{tru} + \kappa_\alpha \sigma_\xi] \tag{32}$$

where ϵ_{tru} is the true (channel) energy amplitude associated with the targeted (for detection) radionuclide, $\xi_\epsilon(n)$ is the raw *EMS* photon arrival amplitude level measurement, κ_α is the respective confidence coefficient with associated confidence level α and σ_ξ is the associated standard deviation associated with the precision of the measurement instrument. When the photon amplitude is accepted as belonging to the *mth*-channel, then $\xi_{\epsilon_m} \rightarrow \epsilon_m(n)$ and the interarrival measurement time-tag is tested similarly for validity by the following confidence interval discriminator[2]

$$[\triangle\tau_{tru} - \kappa_{\tilde{\alpha}}\sigma_{\triangle\tau} \leq \triangle\hat{\tau}_m(n) \leq \triangle\tau_{tru} + \kappa_{\tilde{\alpha}}\sigma_{\triangle\tau}] \qquad (33)$$

where $\triangle\tau_{tru}$ is the true (channel) interarrival amplitude associated with the targeted (for detection) radionuclide, $\xi_{\triangle\tau}(n)$ is the raw *EMS* photon interarrival measurement, $\kappa_{\tilde{\alpha}}$ is the respective confidence coefficient with associated confidence level $\tilde{\alpha}$ and $\sigma_{\triangle\tau}$ is the standard deviation with the variance of the interarrival. Since the estimated interarrival time ($\triangle\hat{\tau}_m$) is *not* the actual source interarrival, we use a simple transport model with calibration data obtained prior to actual deployment processing.

After discrimination, we raw measurements are then processed using the Bayesian techniques, the linear Kalman filter (*LKF*) and the particle filter (*PF*) developed in the previous section [4]. However, if the time-tag does *not* match the true, then photon is *rejected* and no further processing occurs. The branching or occurrence probability is estimated using counting methods as discussed next.

2) Probability of Occurrence Estimation: We use a simple counting technique to estimate the branching or occurrence probability parameters. At each accepted arrival (after discrimination). the counting estimator for the *mth*-monoenergetic component of the radionuclide is given by

$$\hat{\alpha}_m(n) = \frac{N_{\epsilon_m}(n)}{M_\epsilon(n)} \qquad (34)$$

where $N_{\epsilon_m}(n)$ is the total counts for the *mth* source at arrival time n or simply the *mth-channel count* and $M_\epsilon(n)$ is the *total count* of all of the RN channels or monoenergetic sources at n. Note that $N_{\epsilon_m}(n)$ is updated by arrivals on channels corresponding to the targeted RN so that at each new channel arrival we have $\{\epsilon_m(n), \triangle\tau_m(n)\} \rightarrow \{\epsilon_m(n+1), \triangle\tau_m(n+1)\}$ such that $N_{\epsilon_m}(n+1) \rightarrow N_{\epsilon_m}(n)+1; M_\epsilon(n+1) \rightarrow M_\epsilon(n)+1$ and $\hat{\alpha}_m(n+1) \rightarrow \hat{\alpha}_m(n)$.

3) Energy Amplitude Level/Interarrival (Rate) Bayesian Parameter Estimation Results: As each photon is acquired, the measurement and arrival times are extracted and discriminated. If accepted then both the associated energy amplitude level and interarrival time are sequentially updated using the *LKF* processor for the amplitude and *PF* processor for the interarrival time. A typical result of the processing for an entire run is shown in Fig. 4 for a cesium radionuclide (^{137}Cs). In $4a$ we set the energy amplitude level estimate and its zero-mean/whiteness test in Fig. $4b$. Recall that for a *LKF* processor the resulting innovations sequence must be zero-mean and white (uncorrelated). This is the case for the energy amplitude estimates with $(8.7 \times 10^{-19} < 3.1 \times 10^{-2})/0.1\%$ out) as illustrated in the figure. The interarrival estimates are also reasonable and the zero-mean/whiteness check validates its performance with $(8.3 \times 10^{-4} < 3.1 \times 10^{-2})/4\%$ out) quite good. In summary both estimators perform reasonably and are

[2]For large n, the estimate is approximately Gaussian, $\triangle\hat{\tau} \sim \mathcal{N}(\lambda, \lambda/\sqrt{n})$.

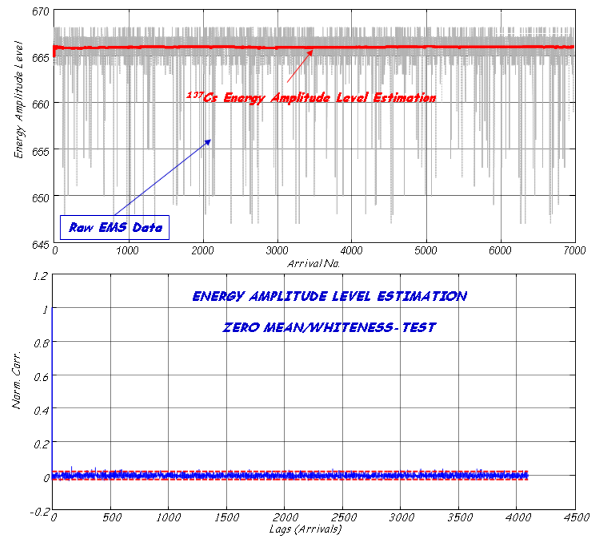

Fig. 4. Bayesian model-based processing for ^{137}Cs radionuclide: (a) Photon energy amplitude levels estimates (*LKF*). (b) Zero-mean/whiteness testing $(8.7 \times 10^{-19} < 3.1 \times 10^{-2})/0.1\%$ out).

checked for validity by performing statistical whiteness tests which are optimal in the *LKF* case and reasonable for the *PF* case ([3],[4]).

The experimental set-up consists of sources, measurement instruments (some for monitoring) including a high purity germanium (HPG) commercial detector. The sources consisted of a set of known calibration sources with multiple energy lines and unknown background sources as shown in the *PHS* of Fig. 5a. The results of the processing using the parallel/distributed processing scheme described in the previous sections are shown in Fig. 5b where we see the raw *PHS* measured by the commercial instrumentation as well as that by the sequential Bayesian processor. Clearly, the sequential processor is capable of performing the estimation quite well as demonstrated previously on the cesium source (see Fig. 4). Its *PHS* is uncluttered with undesirable energy counts and background primarily due to the processing scheme demonstrating its effectiveness over this controlled experimental data set.

4) Sequential Radionuclide Detection/Classification: The sequential radionuclide detector is constructed as discussed in Sec. 4.1 and Eq. 23. However, it is implemented in a channel-by-channel framework as depicted in Fig. 3. Basically, the individual distributions are calculated in *parallel* at each channel and then combined in the detector/classifier as illustrated for the specific distributions where the required parameters are replaced by their estimates. At each arrival after discrimination, the accepted channel photon, say jth is processed by the energy amplitude level and interarrival parameter estimators ($\hat{\theta}$) providing the input to the likelihood ratio along with the truth parameters (θ^t) available from the tables [2] to give $[\{\epsilon^t_m\}, \{\triangle\tau^t_m\}, \{\alpha^t_m\}]$; $m = 1, \cdots, M_\epsilon$. Using the distribution relations developed for the joint parametric distributions, and simplifying notation, we define the following

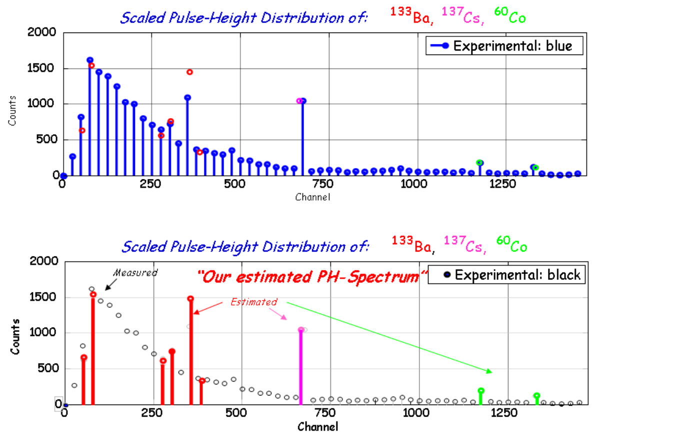

Fig. 5. Results of Bayesian parameter estimation for ^{133}Ba,^{137}Cs, ^{60}Co radionuclides: (a) *PHS* estimation using high precision HGe commercial detector. (b) Parallel/distributed Bayesian processor using *LKF* and *PF* parameter estimators.

general functional form

$$\Theta_m(n;\theta) := \Pr(\triangle\tau_m(n)|\mathcal{I}_m(k),\Xi_{n-1},\mathcal{H}_\ell)\times \Pr(\epsilon_m(n)|\mathcal{I}_m(k),\Xi_{n-1},\mathcal{H}_\ell)\times\Pr(\mathcal{I}_m(k)|\Xi_{n-1},\mathcal{H}_\ell) \tag{35}$$

and for our specific problem, we have under hypothesis $\mathcal{H}_0$

$$\Theta_m(n;\hat{\theta}) = \frac{\hat{\alpha}_m\hat{\lambda}_{\triangle\tau_m}(n|n)}{\sqrt{2\pi}\hat{\sigma}_{\epsilon_m}(n|n)}\exp\left\{-\hat{\alpha}_m\hat{\lambda}_{\triangle\tau_m}(n|n)\times \triangle\tau_m(n)-\frac{(\epsilon_m(n)-\hat{\epsilon}_m(n|n))^2}{2\hat{\sigma}^2_{\epsilon_m}(n|n)}\right\} \tag{36}$$

and under hypothesis $\mathcal{H}_1$

$$\Theta_m(n;\theta^t) = \frac{\alpha_m^t\lambda^t_{\triangle\tau_m}}{\sqrt{2\pi}\sigma_{\epsilon_m^t}}\times \exp\left\{-\alpha_m^t\lambda^t_{\triangle\tau_m}\triangle\tau_m(n)-\frac{(\epsilon_m(n)-\epsilon_m^t)^2}{2\sigma^2_{\epsilon_m^t}}\right\} \tag{38}$$

Therefore, we can re-write Eq. 23 using this notation simply as:

$$\Lambda[\Xi_n] = \Lambda[\Xi_{n-1}] + \sum_{m=1}^{M_\epsilon}\ln\Theta_m(n;\theta^t) - \sum_{m=1}^{M_\epsilon}\ln\Theta_m(n;\hat{\theta}) \tag{39}$$

Combining similar terms, we obtain the final sequential log-likelihood ratio radionuclide detector specified by:

$$\Lambda[\Xi_n] = \Lambda[\Xi_{n-1}] + \sum_{m=1}^{M_\epsilon}\ln\left(\frac{\alpha_m^t\lambda^t_{\triangle\tau_m}}{\sqrt{2\pi}\sigma_{\epsilon_m^t}}\right) - \ln\left(\frac{\hat{\alpha}_m\hat{\lambda}_{\triangle\tau_m}(n|n)}{\sqrt{2\pi}\hat{\sigma}_{\epsilon_m}(n|n)}\right) + \left(\hat{\alpha}_m\hat{\lambda}_{\triangle\tau_m}(n|n)-\alpha_m^t\lambda^t_{\triangle\tau_m}\right)\times\triangle\tau_m(n) + \frac{1}{2}\left(\frac{\epsilon_m(n)-\hat{\epsilon}_m(n|n)}{\hat{\sigma}_{\epsilon_m}(n|n)}\right)^2 - \frac{1}{2}\left(\frac{\epsilon_m(n)-\epsilon_m^t(n)}{\sigma_{\epsilon_m^t}}\right)^2 \tag{40}$$

with implementation depicted in the figure where we observe that after successful discrimination the parameters are estimated and employed to calculate the log-likelihood function as in Eq. 40. These are estimated channel-by-channel (mth-channel) and the overall decision function implemented sequentially (in arrival time). The diagram shows the input photon measurement data (raw amplitude/interarrival) *after* discrimination as input to the individual channel parameter estimators. Once the parameters are estimated they are implemented in each channel log-likelihood partial calculation ($\Theta_m(n;\theta)$) and all of the partial sums are combined along with the previous (in arrival time) log-likelihood to sequentially update the new log-likelihood at time n. It is then compared to the threshold to see if a detection is possible. If not, the next photon is processed and the log-likelihood updated to see if a decision can be made. This sequential radionuclide process continues until there is enough data for a decision to made.

V. Proof-of-Principle Experiment

The sequential Bayesian detector was applied to a set of experimental composite radionuclide *EMS* data consisting of three radionuclides cobalt (^{60}Co), cesium (^{137}Cs), barium (^{133}Ba) with 2, 1 and 5 energy lines (monoenergetic sources), respectively along with background and an extraneous potassium source. The sequence and corresponding pulse-height spectrum is shown in Fig. 5. In (a) we observe the measured photon energy amplitudes with the *PHS* shown in (b). The primary objective was to assess the performance of the processor along with ability to detect and classify targeted radionuclides. After an initial calibration phase of the algorithm which consisted of "tuning" the Bayesian processors on simulated and controlled data, setting initial parameters, etc., the overall results of the processing are shown in Fig. 6. We note four columns of data, the first column is the composite pulse-height spectrum, with the second the composite *EMS* with the circles representing the *discriminator* output photons. Notice that they are chosen by the discriminator confidence intervals for *both* energy amplitude and the corresponding time-tag and align with the photo-peak bins of the *PHS*. The third column represents the enhanced energy amplitude levels of the processed (channel) photon while the final column is the likelihood decision functions for each of the targeted radionuclides. As each photon is processed, the decision function is sequentially updated until one of the thresholds (target/nontarget) is crossed (lighter crosses in figure) declaring a threat or non-threat. Note that the barium is detected (threshold exceeded) first (0.78 secs) followed by the cesium (1.0 sec) and then cobalt (4 sec). It is interesting to note that the decision function is using all of the available information extracted from the *EMS*.

It should also be noted that the thresholds are determined from a receiver operating characteristic (*ROC*) curve for each radionuclide decision function. That is, we synthesize *EMS* and noise sequences using a brute force approach to estimating the *ROC* curves in order to calculate the required thresholds.

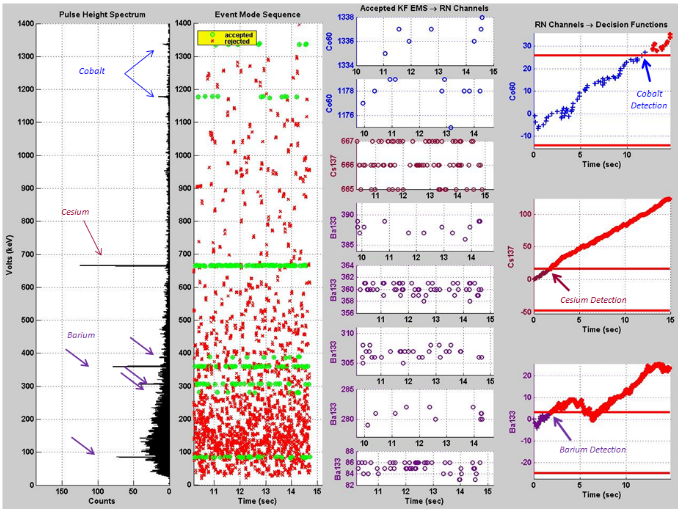

Fig. 6. Sequential Bayesian detection and classification. (a) Pulse-height spectrum (after calibration). (b) *EMS* with discrimination (circles). (c) Enhanced energy amplitude levels. (d) Log-likelihood decision functions for cobalt 60, cesium 137 and barium 133 radionuclide detection/classification.

Based on the selected detection and false-alarm probabilities respectively, (98%, 2%), the thresholds corresponding to this operating point were calculated according to Eq. 10 for each radionuclide.

VI. Summary

We have shown that a sequential Bayesian detector can be developed to solve the radiation detection problem by defining a target radionuclide(s) and its monoenergetic decomposition model evolving from the underlying transport physics of the photon and measurement process. We developed a Bayesian probabilistic framework to theoretically define and solve the problem. Under certain assumed distributions, a particular realization of the process was successfully developed and applied to experimental data demonstrating its overall performance.

VII. Acknowledgments

We would like to acknowledge the contributions of our nuclear experts, Dr. T. Gosnell, Dr. D. Slaughter and Professor S. Prussin. This work performed under the auspices of the U.S. Department of Energy by Lawrence Livermore National Laboratory under Contract DE-AC52-07NA27344.

References

[1] R. D. Evans, *The Atomic Nucleus.* New York, New York: McGraw-Hill, 1985.

[2] G.F. Knoll, *Radiation Detection and Measurement*, 3rd ed., Hoboken New Jersey: John Wiley, 2000.

[3] J. V. Candy, *Model-Based Signal Processing*, Hoboken, New Jersey: John Wiley/IEEE Press, 2006.

[4] J. V. Candy, *Bayesian Signal Processing, Classical, Modern and Particle Filtering*, Hoboken New Jersey: John Wiley/IEEE Press, 2009.

[5] S. Haykin and N. de Freitas, "Special Issue, Sequential state estimation, from Kalman filters to particle filters," *Proc. IEEE*, vol. 92, no. 3, pp. 399-574, 2004.

[6] D. L. Snyder and M. I. Miller, *Random Point Process in Time and Space.* New York, New York: Springer-Verlag, 1991.

[7] C. Andrieu, E. Barat and A. Doucet, Bayesian deconvolution of noisy filtered point processes, *IEEE Trans. Sig. Proc.*, Vol. 49, pp. 134-146, 2001.

[8] S. Gulam Razul, W. J. Fitzgerald and C. Andrieu, Bayesian model selection and parameter estimation of nuclear emission spectra using RJMCMC, Nucl. Instrum. And Methods in Physics Res. A, Vol. 497, pp. 492-510, 2003.

[9] D. Chambers, "A signal processing model for radiation transport," **LLNL Report**, LLNL-TR-405952, 2008.

[10] K. Sale, J. Candy, E. Breitfeller, B. Guidry, D. Manatt, T. Gosnell and D. Chambers, "A Bayesian sequential approach to spectroscopic portal system decisions" *SPIE Confr. Proceed.*, pp. 1-23, 2007.

[11] J. Candy, K. Sale, B. Guidry, E. Breitfeller, D. Manatt, D. Chambers and A. Meyer, "Bayesian processing for the detection of radiactive contraband from uncertain measurements," *IEEE CAMSAC Confr.*, pp. 2-6, 2007.

[12] A. Papoulis and S. Pillai, *Probability, Random Variables and Stochastic Processes*, 4th ed., New York, New York: McGraw-Hill, 2002.

[13] J. Liu, *Monte Carlo Strategies in Scientific Computing*, New York, New York: Springer-Verlag, 2001.

[14] H. Van Trees, *Detection, Estimation and Modulation Theory*, pt. 1, New York, New York: John Wiley, 1968.

[15] A. Wald, *Sequential Analysis*, New York, New York: Dover Publications, 1973.

[16] A. Doucet, N. de Freitas and N. Gordon, *Sequential Monte Carlo Methods in Practice*, New York, New York: Springer-Verlag, 2001.

[17] B. Ristic B., S. Arulampalam and N. Gordon, *Beyond the Kalman Filter, Particle Filters for Tracking Applications*, Boston, Massachusetts: Artech House, 2004.

[18] S. Godsill and P. Djuric, "Special Issue, Monte Carlo methods for statistical signal processing," *IEEE Trans. Signal Proc.*, vol. 50, pp. 173-499, 2002.

[19] P. Djuric, J. Kotecha, J. Zhang, Y. Huang, T. Ghirmai, M. Bugallo and J. Miguez, "Particle Filtering," *IEEE Signal Proc. Mag.* vol. 20, no. 5, pp. 19-38, 2003.

[20] J. V. Candy, "Bootstrap particle filtering," *IEEE Signal Proc. Mag.* vol. 24, no. 4, pp. 73-85, 2007.